Volume 1 Subject Index 1992

Alclad

Comparison of Corrosion-Fatigue Properties of 6013 Bare Alclad 2024 and 2024 Bare Aluminum Alloy Sheet Materials 1,1; 91-96

Alloying, mechanical

New Permanent Magnets and New Processing Techniques 1,2; 175-181

Rare-Earth Nitrides and Carbides: A New Class of Permanent Magnet Materials 1,2; 193-203

Effects of Processing Parameters in P/M Steel Forging on Part Properties: A Review Part I: Preparation, Compaction, and Sintering 1,4; 495-503

Effects of Processing Parameters in P/M Steel Forging on Part Properties: A Review Part II: Forging of Sintered Compact 1,4; 505-516

Effects of Processing Parameters in P/M Steel Forging on Part Properties: A Review Part III: Analysis Methods 1,4; 517-530

Aluminum

Effects of Electrodeposited Zinc Coating on the Formability of Drawing-Quality Aluminum-Killed Sheet Steel 1,2; 275-283

An Investigation into the Production of Bi- and Tri-Layered Strip by Drawing through Wedge-Shaped Dies 1,2; 285-291

Metallurgical Stability and the Fracture Behavior of Ferritic Stainless Steels 1,3; 371-382

Fracture and Mechanical Properties of P100 Gr/6061 Al Composite 1,4; 463-467

Aluminum alloys

A Statistical Approach to the Heat Treatment Optimization of Al-Al_2O_3Particulate Composites 1,1; 45-48

Effects of Spray Configuration on the Uniformity of Cooling Rate and Hardness in the Quenching of Aluminum Parts with Non-Uniform Shapes 1,1; 49-60

Effect of Suspended Solids on the Flow-Induced Corrosion of a Modified Al-2.5Mg Alloy in Arabian Gulf Water 1,1; 61-66

Comparison of Corrosion-Fatigue Properties of 6013 Bare, Alclad 2024, and 2024 Bare Aluminum Alloy Sheet Materials 1,1; 91-96

Analysis of the Central Cavity of Axisymmetric Forward Extrusion by the Upper Bound Approach 1,3; 409-413

Elimination of Porosity from Aluminum-Silicon Castings by Hot Isostatic Pressing 1,6; 773-780

Effects of Cutting Conditions on Drilling of Aluminum 380 1,6; 797-800

Some Observations on Hardness Measurements of Particulate-Reinforced 6061 Aluminum Metal Matrix Composites 1,6; 839-844

A Study of Nitrogen Ion-Implanted Ti-6Al-4V ELI by Plasma Source Ion Implantation at High Temperature 1,6; 845-848

Analysis

Damping Characteristics of Composite Materials and Structures 1,1; 11-20

Effects of Processing Parameters in P/M Steel Forging on Part Properties: A Review Part III: Analysis Methods 1,4; 517-530

Interface Friction and Deformation Kinematics in Metal Compression with Sticking Friction 1,4; 531-541

See also Computer program
Thermomagnetic

Bearings

Modeling and Analysis of Journal Bearings Lubricated with Molten Zinc for Galvanizing Process 1,3; 323-331

Bending

Technical Note: A New Test Procedure for the Bending Under Tension Friction Test 1,5; 609-613

Application of the Bending-Under-Tension Friction Test to Coated Sheet Steels 1,5; 685-693

Specimen Edge Effects on Bending Fatigue of Carburized Steel 1,5; 695-703

Bonding

Low-Temperature Solid State Bonding of Copper 1,1; 35-44

Boron alloys

Permanent Magnetic Materials—Developments During the Past 12 Months 1,2; 167-174

Calcium

Effect of Rare Earth and Calcium Treatments on the Mechanical, Physical, and Electrochemical Properties of a 16Mn Steel 1,1; 21-27

Carburization

Effect of H_2O Contents in Air on the Carbonizing Behavior of Charcoal Gas 1,3; 383-391

Casting

Elimination of Porosity from Aluminum-Silicon Castings by Hot Isostatic Pressing 1,6; 773-780

Ceramic materials

Pressureless Sintered High-Strength Mullite from Commercial Powder 1,4; 543-546

Characterization

Damping Characteristics of Composite Materials and Structures 1,1; 11-20

Effect of Rare Earth and Calcium Treatments on the Mechanical, Physical, and Electrochemical Properties of a 16Mn Steel 1,1; 21-27

Chromium

Use of Nitrogen-Implanted Chromium Overcoat for Improving the Durability of Thin-Film Magnetic Media 1,4; 489-493

Chromium alloys

Oxidation at Defects in Scales on Iron-Chromium Alloys 1,1; 75-82

The Relationship Between the Minimum Creep Rate and the Rupture Time in Cr-Mo Steels 1,1; 123-128

Stress-Corrosion Cracking of 15Cr-15Ni-2.2Mo Titanium-Modified Austenitic Stainless Steels 1,6; 823-830

Claddings

Comparison of Corrosion-Fatigue Properties of 6013 Bare, Alclad 2024, and 2024 Bare Aluminum Alloy Sheet Materials 1,1; 91-96

Coatings

The Relationship Between the Minimum Creep Rate and the Rupture Time in Cr-Mo Steels 1,1; 123-128

The Influence of Composition and Processing Parameters on the Mechanical Properties and Erosion Response of Ni + TiB_2 Coatings 1,1; 129-142

Effects of Electrodeposited Zinc Coating on the Formability of Drawing-Quality Aluminum-Killed Sheet Steel 1,2; 275-283

An Investigation into the Production of Bi- and Tri-Layered Strip by Drawing through Wedge-Shaped Dies 1,2; 285-291

Electroplating of Ni-Cr on Steel with Pulse Plating 1,3; 359-361

Cobalt alloys

Permanent Magnetic Materials—Developments During the Past 12 Months 1,2; 167-174

Composite materials

Predictive Creep Response of Linear Viscoelastic Graphite/Epoxy Composites Using the Laplace Transform Method 1,2; 261-256

An Investigation into the Production of Bi- and Tri-Layered Strip by Drawing through Wedge-Shaped Dies 1,2; 285-291

Fracture and Mechanical Properties of P100 Gr/6061 Al Composite 1,4; 463-467

See also Copper alloys
Damping
Metal matrix

Composites

Effects of Heat Treatment on the Mechanical Properties of SiC_p/6061 Al Composite 1,5; 615-629

Computer analysis

Recent Progress in 2:17-Type Permanent Magnets 1,2; 183-191

Computer program

A Statistical Approach to the Heat Treatment Optimization of Al-Al_2O_3 Particulate Composites 1,1; 45-48

Effects of Spray Configuration on the Uniformity of Cooling Rate and Hardness in the Quenching of Aluminum Parts with Non-Uniform Shapes 1,1; 49-60

Pictorial Representation of Solid-Gas Equilibria at High Temperatures 1,1; 83-89

Finite-Element Simulation of Induction Heat Treatment 1,1; 97-112

Importance of Rotational Losses in Rotating Machines and Transformers 1,2; 235-244

Predictive Creep Response of Linear Viscoelastic Graphite/Epoxy Composites Using the Laplace Transform Method 1,2; 261-256

Creep Life Prediction of Low-Alloy Steels Basd on the β-Envelope Method 1,3; 333-340

Analysis of the Central Cavity of Axisymmetric Forward Extrusion by the Upper Bound Approach 1,3; 409-413

A Knowledge-Based System for Generation and Control of Finite-Element Meshes in Forging Simulation 1,3; 415-428

Isothermal and Thermomechanical Finite-Element Analysis of the Tube Drawing Process Using a Fixed Tapered Plug 1,4; 547-554

Cooling
Cooling Strategies for Cryogenic Machining from a Materials Viewpoint 1,5; 669-678

Copper
Low-Temperature Solid State Bonding of Copper 1,1: 35-44
Isothermal and Thermomechanical Finite-Element Analysis of the Tube Drawing Process Using a Fixed Tapered Plug 1,4; 547-554

Copper alloys
Heat Resistant Dispersion-Strengthened Copper Alloys 1,1; 113-121

Corrosion
Effect of Suspended Solids on the Flow-Induced Corrosion of a Modified Al-2.5Mg Alloy in Arabian Gulf Water 1,1: 61-66
Comparison of Corrosion-Fatigue Properties of 6013 Bare, Alclad 2024, and 2024 Bare Aluminum Alloy Sheet Materials 1,1: 91-96
Intergranular Corrosion Resistance of Microstructure-Modified Type 316 Austenitic Stainless Steel 1,6; 831-838
Permanent Magnetic Materials—Developments During the Past 12 Months 1,2; 167-174
Improving Intergranular Corrosion Resistance of Sensitized Type 316 Austenitic Stainless Steel by Laser Surface Melting 1,3; 341-345
Effect of H_2O Contents in Air on the Carbonizing Behavior of Charcoal Gas 1,3; 383-391
Review of Metals and Binary Oxides as Sorbents for Removing Sulfur from Coal-Derived Gases 1,3; 399-407
Mechanical Properties of Haynes Alloy 188 after Exposure to LiF-22CaF_2, Air, and Vacuum at 1093 K for Periods up to 10,000 Hours 1,4; 469-482
Custom Age 625® Plus Alloy—A Higher Strength Alternative to Alloy 625 1,4; 483-488
Stress-Corrosion Cracking of 15Cr-15Ni-2.2Mo Titanium-Modified Austenitic Stainless Steels 1,6; 823-830

Cracking
See Corrosion

Creep
The Relationship Between Minimum Creep Rate and the Rupture Time in Cr-O Steels 1,1; 123-128
Predictive Creep Response of Linear Viscoelastic Graphite/Epoxy Composites Using the Laplace Transform Method 1,2; 261-256
Creep Life Prediction of Low-Alloy Steels Basd on the β-Envelope Method 1,3; 333-340

Cryogenic
Cooling Strategies for Cryogenic Machining from a Materials Viewpoint 1,5; 669-678
Cryogenic Properties of Some Cutting Tool Materials 1,5; 705-714

Cutting
Effects of Cutting Conditions on Drilling of Aluminum 380 1,6; 797-800

Damping
Damping Characteristics of Composite Materials and Structures 1,1: 11-20

Deformation
Interface Friction and Deformation Kinematics in Metal Compression with Sticking Friction 1,4; 531-541

Densification
Densification of Titanium Diboride by Hot Isostatic Pressing and Production of Near-Net-Shape Components 1,5; 625-636

Drawing
Effects of Electrodeposited Zinc Coating on the Formability of Drawing-Quality Aluminum-Killed Sheet Steel 1,2; 275-283
An Investigation into the Production of Bi- and Tri-Layered Strip by Drawing through Wedge-Shaped Dies 1,2; 285-291
Isothermal and Thermomechanical Finite-Element Analysis of the Tube Drawing Process Using a Fixed Tapered Plug 1,4; 547-554

Drilling
Effects of Cutting Conditions on Drilling of Aluminum 380 1,6; 797-800

Economics
Energy-Efficient Steels for Motor Laminations 1,2; 227-234

Electrical
Fabrication and Properties of Thin-Film Heterostructures: High Temperature Superconductor/Solid Electrolyte/Electrodes 1,1: 9-10

Electrochemical, properties
Effect of Rare Earth and Calcium Treatments on the Mechanical, Physical, and Electrochemical Properties of a 16Mn Steel 1,1: 21-27

Electrochemical, testing
Effect of Suspended Solids on the Flow-Induced Corrosion of a Modified Al-2.5Mg Alloy in Arabian Gulf Water 1,1: 61-66

Electrodeposition
Effects of Electrodeposited Zinc Coating on the Formability of Drawing-Quality Aluminum-Killed Sheet Steel 1,2; 275-283

Electroplating
Electroplating of Ni-Cr on Steel with Pulse Plating 1,3; 359-361

Emissivity
High-Temperature Spectral Emissivity of Several Refractory Elements and Alloys 1,5; 679-684

Energy
Review of Metals and Binary Oxides as Sorbents for Removing Sulfur from Coal-Derived Gases 1,3; 399-407
Custom Age 625® Plus Alloy—A Higher Strength Alternative to Alloy 625 1,4; 483-488
Thermodynamic Analysis of Sorption Reactions for the Removal of Sulfur from Hot Gases 1,4; 565-571

Energy, thermal
Compatibility of Inconel 617® Alloy with LiF-MgF2-KF Thermal Energy Storage Salts and Vacuum at High Temperature 1,6; 755-762

Erosion
The Influence of Composition and Processing Parameters on the Mechanical Properties and Erosion Response of Ni + TiB_2 Coatings 1,1; 129-142

Equilibria
Pictorial Representation of Solid-Gas Equilibria at High Temperature 1,1: 83-89

Extrusion
Analysis of the Central Cavity of Axisymmetric Forward Extrusion by the Upper Bound Approach 1,3; 409-413

Extruaion, cold
Mechanical and Fatigue Properties of Stress Relieved Type 302 Stainless Steel Wire 1,3; 363-369

Fabrication
Fabrication and Properties of Thin-Film Heterostructures: High-Temperature Superconductor/Solid Electrolyte/Electrodes 1,1: 9-10

Fatigue
Comparison of Corrosion-Fatigue Properties of 6013 Bare, Alclad 2024, and 2024 Bare Aluminum Alloy Sheet Materials 1,1: 91-96
Fatigue Crack Growth Behavior of a Solid Solution-Strengthened Nickel-Base Superalloy (Incoloy 825) 1,1: 67-74
An On-Line Grain Size Measuring System for Grain-Oriented Steels 1,2; 245-248
Detection of Fatigue in Strucutral Steels by Magnetic Property Measurements 1,2; 249-253

Films
Use of Nitrogen-Implanted Chromium Overcoat for Improving the Durability of Thin-Film Magnetic Media 1,4; 489-493

Films, thin
Fabrication and Properties of Thin-Film Heterostructures: High Temperature Superconductor/Solid Electrolyte/Electrodes 1,1: 9-10

Finite element
A Knowledge-Based System for Generation and Control of Finite-Element Meshes in Forging Simulation 1,3; 415-428

Flow, fluid
Three-Dimensional Mathematical Modeling of Fluid Flow in Slab Tundishes and Its Verification with Water Model Experiments 1,5; 625-636
Modeling of the Flow Distribution in an Oil Quench Tank 1,6; 781-788

Fluorine
Compatibility of Inconel 617® Alloy with LiF-MgF2-KF Thermal Energy Storage Salts and Vacuum at High Temperature 1,6; 755-762

Forging
A Knowledge-Based System for Generation and Control of Finite-Element Meshes in Forging Simulation 1,3; 415-428
Effects of Processing Parameters in P/M Steel Forging on Part Properties: A Review Part II: Forging of Sintered Compact 1,4; 505-516

Forming
Effects of Electrodeposited Zinc Coating on the Formability of Drawing-Quality Aluminum-Killed Sheet Steel 1,2; 275-283
See also Sheet

Forming, sheet
Determination of Frictional Behavior in Sheet Metals Using Orthogonal Arrays 1,4; 555-564

Fracture
Metallurgical Stability and the Fracture Behavior of Ferritic Stainless Steels 1,3; 371-382
Fracture and Mechanical Properties of P100 Gr/6061 Al Composite 1,4; 463-467
Effects of Processing Parameters in P/M Steel Forging on Part Properties: A Review Part I: Preparation, Compaction, and Sintering 1,4; 495-503
Effects of Processing Parameters in P/M Steel Forging on Part Properties: A Review Part II: Forging of Sintered Compact 1,4; 505-516

Effects of Processing Parameters in P/M Steel Forging on Part Properties: A Review Part III: Analysis Methods 1,4; 517-530
Pressureless Sintered High-Strength Mullite from Commercial Powder 1,4; 543-546
On Plastic Zones and Fracture Strengths in Some Metal Matrix Composites 1,5; 659-668

Friction

Technical Note: A New Test Procedure for the Bending Under Tension Friction Test 1,5; 609-613
Application of the Bending-Under-Tension Friction Test to Coated Sheet Steels 1,5; 685-693
Specimen Edge Effects on Bending Fatigue of Carburized Steel 1,5; 695-703

Galvanizing

Modeling and Analysis of Journal Bearings Lubricated with Molten Zinc for Galvanizing Process 1,3; 323-331

Grain

High-Resolution Electron Microscope Study of the Grain Boundary Phase in Rapidly Quenched Nd-Fe-B Permanent Magnet Alloys 1,2; 205-209

See also Grain boundary
Measurement

Grain Size

The Effect of Partial Substitution of Nb for V on Austenite Grain Size and Hardness of a Tool Steel 1,6; 751-754

Hardness

The Effect of Partial Substitution of Nb for V on Austenite Grain Size and Hardness of a Tool Steel 1,6; 751-754
Some Observations on Hardness Measurements of Particulate-Reinforced 6061 Aluminum Metal Matrix Composites 1,6; 839-844

Heat treating

Selective Hardening in E52100 Steel 1,2; 267-274
Mechanical and Fatigue Properties of Stress Relieved Type 302 Stainless Steel Wire 1,3; 363-369
Metallurgical Stability and the Fracture Behavior of Ferritic Stainless Steels 1,3; 371-382
Microstructural Banding in Thermally and Mechanically Processed Titanium 6242 1,3; 393-398
Custom Age 625® Plus Alloy—A Higher Strength Alternative to Alloy 625 1,4; 483-488
Applications of Inverse Techniques to Determine Heat Transfer Coefficients in Heat-Treating Operations 1,6; 763-772

Heat treatment

A Statistical Approach to the heat Treatment Optimization of Al-Al_2O_3 Particulate Composites 1,1; 45-48
Finite-Element Simulation of Induction Heat Treatment 1,1; 97-112
Effects of Heat Treatment on the Mechanical Properties of SiC_p/6061 Al Composite 1,5; 615-629

HIP

Densification of Titanium Diboride by Hot Isostatic Pressing and Production of Near-Net-Shape Components 1,5; 625-636
Elimination of Porosity from Aluminum-Silicon Castings by Hot Isostatic Pressing 1,6; 773-780

Implantation, ion

Use of Nitrogen-Implanted Chromium Overcoat for Improving the Durability of Thin-Film Magnetic Media 1,4; 489-493

Incoloy

Fatigue Crack Growth Behavior of a Solid Solution-Strengthened Nickel-Base Superalloy (Incoloy 825) 1,1; 67-74

Inconel

The Influence of Composition and Processing Parameters on the Mechanical Properties and Erosion Response of Ni + TiB_2 Coatings 1,1; 129-142
Compatibility of Inconel 617® Alloy with LiF-MgF2-K Thermal Energy Storage Salts and Vacuum at High Temperature 1,6; 755-762

Ion-Implantation

A Study of Nitrogen Ion-Implanted Ti-6Al-4V ELI by Plasma Source Ion Implantation at High Temperature 1,6; 845-848

Iron alloys

See Oxidation
Steel
Permanent Magnetic Materials—Developments During the Past 12 Months 1,2; 167-174
Magnetic Properties of High-Efficiency Core Materials NC-M3 and NC-M4 1,3; 219-225

Iron

A New Refining Process for Iron Oxide Using Iron Ore and Its Application 1,2; 211-218

Laminates

Energy-Efficient Steels for Motor Laminations 1,2; 227-234

Laser

Improving Intergranular Corrosion Resistance of Sensitized Type 316 Austenitic Stainless Steel by Laser Surface Melting 1,3; 341-345

Lithium

Compatibility of Inconel 617® Alloy with LiF-MgF2-KF Thermal Energy Storage Salts and Vacuum at High Temperature 1,6; 755-762

Machining

See Cryogenic

Magnesium

Compatibility of Inconel 617® Alloy with LiF-MgF2-KF Thermal Energy Storage Salts and Vacuum at High Temperature 1,6; 755-762

Magnesium alloys

Effect of Suspended Solids on the Flow-Induced Corrosion of a Modified Al-2.5Mg Alloy in Arabian Gulf Water 1,1; 61-66

Magnetic

Effect of Alloying Elements on Response of Non-Oriented Electrical Steels to Stamping Operations 1,1; 29-34

Magnetic materials

Permanent Magnetic Materials—Developments During the Past 12 Months 1,2; 167-174
New Permanent Magnets and New Processing Techniques 1,2; 175-181
Recent Progress in 2:17-Type Permanent Magnets 1,2; 183-191
Rare-Earth Nitrides and Carbides: A New Class of Permanent Magnet Materials 1,2; 193-203
High-Resolution Electron Microscope Study of the Grain Boundary Phase in Rapidly Quenched Nd-Fe-B Permanent Magnet Alloys 1,2; 205-209
A New Refining Process for Iron Oxide Using Iron Ore and Its Application 1,2; 211-218
Magnetic Properties of High-Efficiency Core Materials NC-M3 and NC-M4 1,3; 219-225
Energy-Efficient Steels for Motor Laminations 1,2; 227-234
Importance of Rotational Losses in Rotating Machines and Transformers 1,2; 235-244
An On-Line Grain Size Measuring System for Grain-Oriented Steels 1,2; 245-248
Use of Nitrogen-Implanted Chromium Overcoat for Improving the Durability of Thin-Film Magnetic Media 1,4; 489-493

Measurement

An On-Line Grain Size Measuring System for Grain-Oriented Steels 1,2; 245-248
Detection of Fatigue in Structural Steels by Magnetic Property Measurements 1,2; 249-253

See also Hardess

Mechanical properties

Effect of Rare Earth and Calcium Treatments on the Mechanical, Physical, and Electrochemical Properties of a 16Mn Steel 1,1; 21-27
The Influence of Composition and Processing Parameters on the Mechanical Properties and Erosion Response of Ni + Ti_2 Coatings 1,1; 129-142
Effects of Heat Treatment on the Mechanical Properties of SiC_p/6061 Al Composite 1,5; 615-629

Mechanical testing

The Strength of Nodule-Decorated Whiskers 1,3; 317-322

Metal matrix

A Statistical Approach to the Heat Treatment Optimization of Al-Al^2O_3 Particulate Composites 1,1; 45-48
On Plastic Zones and Fracture Strengths in Some Metal Matrix Composites 1,5; 659-668

Microscopy

Oxidation at Defects in Scales on Iron-Chromium Alloys 1,1; 75-82
High-Resolution Electron Microscope Study of the Grain Boundary Phase in Rapidly Quenched Nd-Fe-B Permanent Magnet Alloys 1,2; 205-209
Microstructural Banding in Thermally and Mechanically Processed Titanium 6242 1,3; 393-398

Microstructure

Intergranular Corrosion Resistance of Microstructure-Modified Type 316 Austenitic Stainless Steel 1,6; 831-838

Modeling

Three-Dimensional Mathematical Modeling of Fluid Flow in Slab Tundishes and Its Verification with Water Model Experiments 1,5; 625-636
Modeling of the Flow Distribution in an Oil Quench Tank 1,6; 781-788

Molybdenum alloys

The Relationship Between the Minimum Creep Rate and the Rupture Time in Cr-Mo Steels 1,1; 123-128
Stress-Corrosion Cracking of 15Cr-15Ni-2.2Mo Titanium-Modified Austenitic Stainless Steels 1,6; 823-830

Mullite

Pressureless Sintered High-Strength Mullite from Commercial Powder 1,4; 543-546

Near-net-shaping
Densification of Titanium Diboride by Hot Isostatic Pressing and Production of Near-Net-Shape Components 1,5; 625-636

Nickel
Review of Metals and Binary Oxides as Sorbents for Removing Sulfur from Coal-Derived Gases 1,3; 399-407

Nickel alloys
Fatigue Crack Growth Behavior of a Solid Solution-Strengthened Nickel-Base Superalloy (Incoloy 825) 1,1; 67-74
Stress-Corrosion Cracking of 15Cr-15Ni-2.2Mo Titanium-Modified Austenitic Stainless Steels 1,6; 823-830

Niobium
The Effect of Partial Substitution of Nb for V on Austenite Grain Size and Hardness of a Tool Steel 1,6; 751-754

Niobium alloys
The Use of Thermoelectric Power (TEP) Measurements to Study Recovery, Recrystallization, and Phase Transformations in Cold-Worked Zr-1%Nb and Zircaloy-4 Nuclear Fuel Sheathing 1,1; 143-148

Nitriding, ion
Geometric Effect of Ion Nitriding on the Nitride Growth Behavior in Hollow Tube 1,3; 353-358

Nitrogen
A Study of Nitrogen Ion-Implanted Ti-6Al-4V ELI by Plasma Source Ion Implantation at High Temperature 1,6; 845-848

Oxidation
Oxidation at Defects in Scales on Iron-Chromium Alloys 1,1; 75-82
Pictorial Representation of Solid-Gas Equilibria at High Temperatures 1,1; 83-89
Effect of H_2O Contents in Air on the Carbonizing Behavior of Charcoal Gas 1,3; 383-391

Oxide
Review of Metals and Binary Oxides as Sorbents for Removing Sulfur from Coal-Derived Gases 1,3; 399-407

See also Iron
Tin

Phase transformations
The User of Thermoelectric Power(TEP) Measurements to Study Recovery, Recrystallization/and Phase Transformations in Cold-Worked Zr-l%Nb and Zircaloy-4 Nuclear Fuel Sheathing 1,1; 143-148

Physical properties
Effect of Rare Earth and Calcium Treatments on the Mechanical, Physical, and Electrochemical Properties of a 16Mn Steel 1,1; 143-148

Plasma deposition
A Study of Nitrogen Ion-Implanted Ti-6Al-4V ELI by Plasma Source Ion Implantation at High Temperature 1,6; 845-848

Plating
Novel Method for Preparation of Silver-Tin Oxide Electrical Contacts 1,2; 255-260

Polymer
See Composite materials

Polymers
Damping Characteristics of Composite Materials and Structures 1,1; 11-20

Porosity
Elimination of Porosity from Aluminum-Silicon Castings by Hot Isostatic Pressing 1,6; 773-780

Powder
Pressureless Sintered High-Strength Mullite from Commercial Powder 1,4; 543-546

Processing
A Statistical Approach to the Heat Treatment Optimization of Al-Al_2O_3 Particulate Composites 1,1; 45-48
Magnetic Properties of High-Efficiency Core Materials NC-M3 and NC-M4 1,3; 219-225
Geometric Effect of Ion Nitriding on the Nitride Growth Behavior in Hollow Tube 1,3; 353-358
Electroplating of Ni-Cr on Steel with Pulse Plating 1,3; 359-361
Interface Friction and Deformation Kinematics in Metal Compression with Sticking Friction 1,4; 531-541
Pressureless Sintered High-Strength Mullite from Commercial Powder 1,4; 543-546
Determination of Frictional Behavior in Sheet Metals Using Orthogonal Arrays 1,4; 555-564

See also Laser
Sputtering
Vacuum

Properties
See Cryogenic
Electrical
Fatigue
Measurement
Mechanical
Magnetic
Physical
Tool, cutting

Quench, oil
Modeling of the Flow Distribution in an Oil Quench Tank 1,6; 781-788

Quenching
See Spray
Rapid

Rare earth
Effect of Rare Earth and Calcium Treatments on the Mechanical, Physical, and Electrochemical Properties of a 16Mn Steel 1,1; 21-27

Rare earths
Permanent Magnetic Materials—Developments During the Past 12 Months 1,2; 167-174
New Permanent Magnets and New Processing Techniques 1,2; 175-181
Recent Progress in 2:17-Type Permanent Magnets 1,2; 183-191
Rare-Earth Nitrides and Carbides: A New Class of Permanent Magnet Materials 1,2; 193-203
High-Resolution Electron Microscope Study of the Grain Boundary Phase in Rapidly Quenched Nd-Fe-B Permanent Magnet Alloys 1,2; 205-209

Recovery
The Use of Thermoelectric Power (TEP) Measurements to Study Recovery, Recrystallization, and Phase Transformations in Cold-Worked Zr-1%Nb and Zircaloy-4 Nuclear Fuel Sheathing 1,1; 143-148

Recrystallization
The Use of Thermoelectric Power (TEP) Measurements to Study Recovery, Recrystallization, and Phase Transformations in Cold-Worked Zr-1%Nb and Zircaloy-4 Nuclear Fuel Sheathing 1,1; 143-148

Refining
A New Refining Process for Iron Oxide Using Iron Ore and Its Application 1,2; 211-218

Refractory
High-Temperature Spectral Emissivity of Several Refractory Elements and Alloys 1,5; 679-684

Reinforcement
The Strength of Nodule-Decorated Whiskers 1,3; 317-322

Rolling
Development of Satellite Mill and Trial Rolling of Profiled Metal Strip 1,6; 789-796

Rupture
The Relationship Between Minimum Creep Rate and the Rupture Time in Cr-Mo Steels 1,1; 123-128

Sheet
Superplastic Sheet Metal Forming of a Generalized Cup—Part 1: Uniform Thinning 1,6; 801-812
Superplastic Sheet Metal Forming of a Generalized Cup—Part 2: Nonuniform Thinning 1,6; 813-822

Silicon
See Casting

Silver alloys
Novel Method for Preparation of Silver-Tin Oxide Electrical Contacts 1,2; 255-260

Slab
Three-Dimensional Mathematical Modeling of Fluid Flow in Slab Tundishes and Its Verificiation with Water Model Experiments 1,5; 625-636

Sorbent
Review of Metals and Binary Oxides as Sorbents for Removing Sulfur from Coal-Derived Gases 1,3; 399-407

Spray quenching
Effects of Spray Configuration on the Uniformity of Cooling Rate and Hardness in the Quenching of Aluminum Parts with Non-Uniform Shapes 1,1; 49-60

Stamping
Effect of Alloying Elements on Response of Non-Oriented Electrical Steels to Stamping Operations 1,1; 21-27

Steel
Effect of Alloying Elements on Response of Non-Oriented Electrical Steels to Stamping Operations 1,1; 29-34
Oxidation at Defects in Scales on Iron-Chromium Alloys 1,1; 75-82
Finite-Element Simulation of Induction Heat Treatment 1,1; 97-112
The Relationship Between Minimum Creep Rate and the Rupture Time in Cr-Mo Steels 1,1; 123-128

Detection of Fatigue in Structural Steels by Magnetic Property Measurements 1,2: 249-253
Selective Hardening in E52100 Steel 1,2: 267-274
Effects of Electrodeposited Zinc Coating on the Formability of Drawing-Quality Aluminum-Killed Sheet Steel 1,2: 275-283
An Investigation into the Production of Bi- and Tri-Layered Strip by Drawing through Wedge-Shaped Dies 1,2: 285-291
Modeling and Analysis of Journal Bearings Lubricated with Molten Zinc for Galvanizing Process 1,3: 323-331
Creep Life Prediction of Low-Alloy Steels Basd on the β-Envelope Method 1,3: 333-340
Improving Intergranular Corrosion Resistance of Sensitized Type 316 Austenitic Stainless Steel by Laser Surface Melting 1,3: 341-345
Geometric Effect of Ion Nitriding on the Nitride Growth Behavior in Hollow Tube 1,3: 353-358
Electroplating of Ni-Cr on Steel with Pulse Plating 1,3: 359-361
Mechanical and Fatigue Properties of Stress Relieved Type 302 Stainless Steel Wire 1,3: 363-369
Metallurgical Stability and the Fracture Behavior of Ferritic Stainless Steels 1,3: 371-382
Effect of H_2O Contents in Air on the Carbonizing Behavior of Charcoal Gas 1,3: 383-391
Determination of Frictional Behavior in Sheet Metals Using Orthogonal Arrays 1,4: 555-564
An On-Line Grain Size Measuring System for Grain-Oriented Steels 1,2: 245-248
Tempering Characteristics of Two Low-Alloy Steels Used for Naval Applications 1,5: 651-657
The Effect of Partial Substitution of Nb for V on Austenite Grain Size and Hardness of a Tool Steel 1,6: 751-754
Stress-Corrosion Cracking of 15Cr-15Ni-2.2Mo Titanium-Modified Austenitic Stainless Steels 1,6: 823-830
Intergranular Corrosion Resistance of Microstructure-Modified Type 316 Austenitic Stainless Steel 1,6: 831-838

Steel processing

Effect of Rare Earth and Calcium Treatments on the Mechanical, Physical, and Electrochemical Properties of a 16Mn Steel 1,1: 21-27

Stress corrosion cracking

Effect of Rare Earth and Calcium Treatments on the Mechanical, Physical, and Electrochemical Properties of a 16Mn Steel 1,1: 21-27

Strip

Development of Satellite Mill and Trial Rolling of Profiled Metal Strip 1,6: 789-796

Strip, layered

An Investigation into the Production of Bi- and Tri-Layered Strip by Drawing through Wedge-Shaped Dies 1,2: 285-291

Substitution

The Effect of Partial Substitution of Nb for V on Austenite Grain Size and Hardness of a Tool Steel 1,6: 751-754

Sulfidation

Pictorial Representation of Solid-Gas Equilibria at High Temperatues 1,1: 83-89

Sulfur, removal

Thermodynamic Analysis of Sorption Reactions for the Removal of Sulfur from Hot Gases 1,4: 565-571

Superalloys

Fatigue Crack Growth Behavior of a Solid Solution-Strengthened Nickel-Base Superalloy (Incoloy 825) 1,1: 67-74

Superconductor

Fabrication and Properties of Thin-Film Heterostructures: High Temperature Superconductor/Solid Electrolyte/Electrodes 1,1: 9-10

Tempering

Tempering Characteristics of Two Low-Alloy Steels Used for Naval Applications 1,5: 651-657

Tensile

Mechanical Properties of Haynes Alloy 188 after Exposure to LiF-22CaF_2, Air, and Vacuum at 1093 K for Periods up to 10,000 Hours 1,4: 469-482
Custom Age 625® Plus Alloy—A Higher Strength Alternative to Alloy 625 1,4: 483-488
Effects of Processing Parameters in P/M Steel Forging on Part Properties: A Review Part I: Preparation, Compaction, and Sintering 1,4: 495-503
Effects of Processing Parameters in P/M Steel Forging on Part Properties: A Review Part II: Forging of Sintered Compact 1,4: 505-516
Effects of Processing Parameters in P/M Steel Forging on Part Properties: A Review Part III: Analysis Methods 1,4: 517-530
Lubrication and Sputtered MoS_2 Films: Principles, Operation, and Limitations 1,3: 347-351

See also Corrosion
Fatigue
Fracture
Mechanical
Tensile

Tensile testing

A Statistical Approach to the Heat Treatment Optimization of Al-Al_2O_3 Particulate Composites 1,1: 45-48

Testing

Lubrication and Sputtered MoS_2 Films: Principles, Operation, and Limitations 1,3: 347-351
Technical Note: A New Test Procedure for the Bending Under Tension Friction Test 1,5: 609-613
Application of the Bending-Under-Tension Friction Test to Coated Sheet Steels 1,5: 685-693
Specimen Edge Effects on Bending Fatigue of Carburized Steel 1,5: 695-703

See also Corrosion
Creep
Erosion
Electrochemical
Fatigue
Fracture
Friction
Mechanical
Rupture
Steel
Tensile
Thermoelectric

Thermoelectric

The Use of Thermoelectric Power (TEP) Measurements to Study Recovery, Recrystallization and Phase Transformations in Cold-Worked Zr-1%Nb and Zircaloy-4 Nuclear Fuel Sheathing 1,1: 143-148

Thermodynamics

Pictorial Representation of Solid-Gas Equilibria at High Temperature 1,1: 83-89
Review of Metals and Binary Oxides as Sorbents for Removing Sulfur from Coal-Derived Gases 1,3: 399-407
Thermodynamic Analysis of Sorption Reactions for the Removal of Sulfur from Hot Gases 1,4: 565-571

Thermomagnetic

Rare-Earth Nitrides and Carbides: A New Class of Permanent Magnet Materials 1,2: 193-203

Thin films

Fabrication and Properties of Thin-Film Heterostructures: High Temperature Superconductor/Solid Electrolyte/Electrodes 1,1: 9-10

Thinning

Superplastic Sheet Metal Forming of a Generalized Cup—Part 1: Uniform Thinning 1,6: 801-812
Superplastic Sheet Metal Forming of a Generalized Cup—Part 2: Nonuniform Thinning 1,6: 813-822

Tin

Novel Method for Preparation of Silver-Tin Oxide Electrical Contacts 1,2: 255-260

Titanium

Microstructural Banding in Thermally and Mechanically Processed Titanium 6242 1,3: 393-398

Titanium alloys

The Influence of Composition and Processing Parameters on the Mechanical Properties and Erosion Response of Ni + TiB_2 Coatings 1,1: 129-142
Densification of Titanium Diboride by Hot Isostatic Pressing and Production of Near-Net-Shape Components 1,5: 637-649
A Study of Nitrogen Ion-Implanted Ti-6Al-4V ELI by Plasma Source Ion Implantation at High Temperature 1,6: 845-848

Tribology

Modeling and Analysis of Journal Bearings Lubricated with Molten Zinc for Galvanizing Process 1,3: 323-331
Lubrication and Sputtered MoS_2 Films: Principles, Operation, and Limitations 1,3: 347-351
Interface Friction and Deformation Kinematics in Metal Compression with Sticking Friction 1,4: 531-541
Determination of Frictional Behavior in Sheet Metals Using Orthogonal Arrays 1,4: 555-564

Tube

Geometric Effect of Ion Nitriding on the Nitride Growth Behavior in Hollow Tube 1,3: 353-358
Isothermal and Thermomechanical Finite-Element Analysis of the Tube Drawing Process Using a Fixed Tapered Plug 1,4: 547-554

Vacuum processing

Low-Temperature Solid State Bonding of Copper 1,1: 35-44

Vanadium

The Effect of Partial Substitution of Nb for V on Austenite Grain Size and Hardness of a Tool Steel 1,6: 751-754

Vanadium Alloys

A Study of Nitrogen Ion-Implanted Ti-6Al-4V ELI by Plasma Source Ion Implantation at High Temperature 1,6: 845-848

Whiskers
The Strength of Nodule-Decorated Whiskers 1,3; 317-322

Wire
Mechanical and Fatigue Properties of Stress Relieved Type 302 Stainless Steel Wire 1,3; 363-369

Zinc
Effects of Electrodeposited Zinc Coating on the Formability of Drawing-Quality Aluminum-Killed Sheet Steel 1,2; 275-283
Modeling and Analysis of Journal Bearings Lubricated with Molten Zinc for Galvanizing Process 1,3; 323-331

Zircaloy
The Use of Thermoelectric Power (TEP) Measurements to Study Recovery, Recrystallization, and Phase Transformations in Cold-Worked Zr-1%Nb and Zircaloy-4 Nuclear Fuel Sheathing 1,1; 143-148

Zirconium alloys
The Use of Thermoelectric Power (TEP) Measurements to Study Recovery, Recrystallization, and Phase Transformations in Cold-Worked Zr-1%Nb and Zircaloy-4 Nuclear Fuel Sheathing 1,1; 143-148

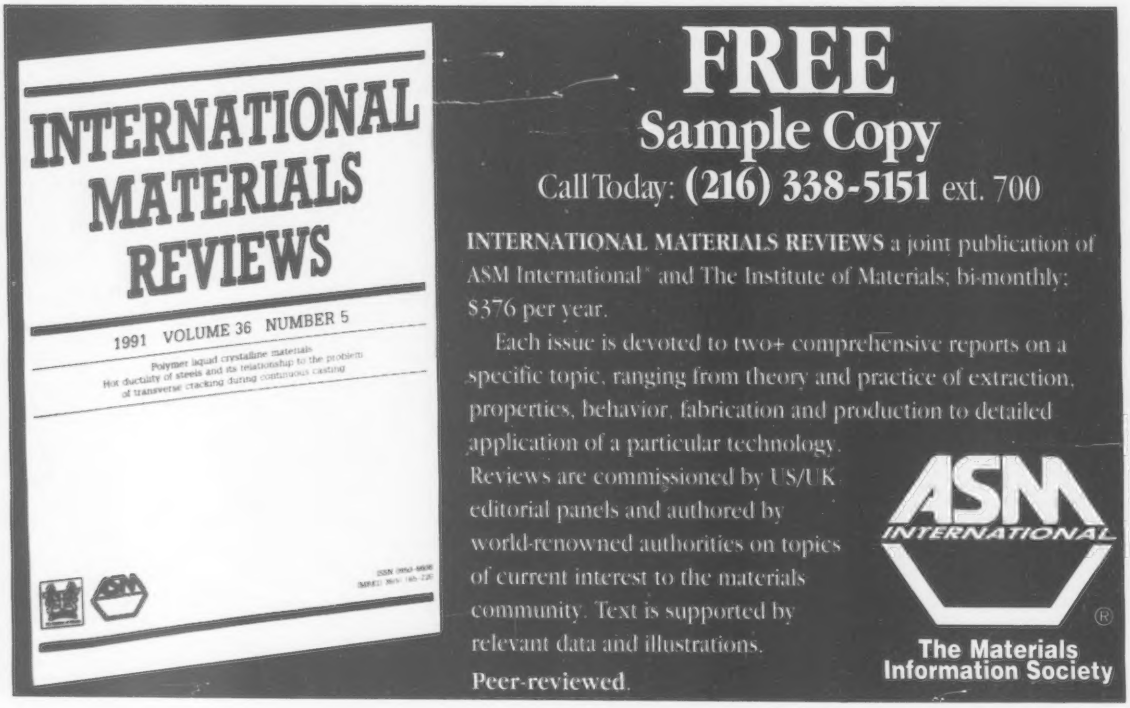
INTERNATIONAL MATERIALS REVIEWS
1991 VOLUME 36 NUMBER 5
Polymer liquid crystalline materials
Hot ductility of steels and its relationship to the problem of transverse cracking during continuous casting
FREE
Sample Copy
Call Today: (216) 338-5151 ext. 700
INTERNATIONAL MATERIALS REVIEWS a joint publication of ASM International® and The Institute of Materials; bi-monthly; $376 per year.
Each issue is devoted to two+ comprehensive reports on a specific topic, ranging from theory and practice of extraction, properties, behavior, fabrication and production to detailed application of a particular technology. Reviews are commissioned by US/UK editorial panels and authored by world-renowned authorities on topics of current interest to the materials community. Text is supported by relevant data and illustrations.
Peer-reviewed.
ASM INTERNATIONAL
The Materials Information Society

Circle (144) on Reader Service Card

Volume 1 Author Index 1992

Abdul Aleem, B.J. 1,1; 61-66
Agarwal, S. 1,4; 489-493
Ahmad, Z. 1,1; 61-66
Aidun, D. 1,4; 463-467
1,5; 615-624
Alexander, G.B. 1,2; 255-260
Baek, W.S. 1,3; 353-358
Bandyopadhyay, S. 1,6; 839-844
Bartosiewicz, L. 1,1; 67-74
Beckley, R. 1,2;245-248
Besson, F. 1,5; 637-649
Bhonsle, S.R. 1,3; 363-369
Biswas, D.K. 1,5; 651-657
Blairs, S. 1,6; 839-844
Blanchard, J. 1,6; 845-848
Boncoeur, M. 1,5; 637-649
Brimacombe, J.K. 1,6; 763-772
Bristow, B.M. 1,3; 393-398
Cameron, J. 1,3; 317-322
Chama, C.C. 1,6; 773-780
Chandra, N. 1,6; 801-812
1,6; 813-822
Chandrasekar, S. 1,1; 97-112
Chang, F.-T. 1,3; 359-361
Chang, H. 1,2; 255-260
Chapman, D. 1,4; 547-554
Chaudhari, J. 1,1; 91-96
Chen, A. 1,6; 845-848
Chen, J. 1,1; 21-27
Chen, Y.-C. 1,3; 383-391
Cho, W.D. 1,1; 75-82
Chou, C.-L. 1,5; 625-636
Chun, C.H. 1,3; 371-382
Cohen, R.E. 1,5; 695-703
Conrad, J.R. 1,4; 489-493
1,6; 845-848
Dabke, P.D. 1,3; 415-428
Das, T. 1,6; 839-844
Dasgupta, D.K. 1,4; 531-541
Dayal, R.K. 1,3; 331-338
1,6; 831-838
DeBold, T.A. 1,4; 483-488
Deshmukh, V.P. 1,5; 651-657
Devine, M.K. 1,2; 249-253
Dodd, R.A. 1,6; 845-848
Duggirala, R. 1,4; 495-503
1,4; 505-516
1,4; 517-530
Edwards, G.R. 1,1; 35-44
Eftekhari, A. 1,1; 91-96
Elias, C.N. 1,6; 751-744
Eldridge, T.W. 1,6; 797-800
Ennis, P.J. 1,3; 333-340
Fetherston, P. 1,6; 845-848
Frank, R.B. 1,4; 483-488
Garwood, D.R. 1,6; 781-788
Giacobbe, F.W. 1,2; 267-274
Gibson, R.F. 1,1; 11-20
Gnanamoorthy, J.B. 1,6; 823-830
Graham, Jr., C.D. 1,2; 205-209
Gremenok, V.F. 1,1; 9-10
Groza, J. 1,1; 113-121
Hadjipanayis. G.C. 1,2; 193-203
Han, S.H. 1,6; 845-848
Haque, I. 1,3; 415-428
Harshe, G. 1,1; 83-89
Hawbolt, E.B. 1,6; 763-772
Henig, E.-Th. 1,2; 167-174
Hernandez-Morales, B. 1,6; 763-772
Hiatt, D.R. 1,3; 393-398
Hirose, S. 1,2; 211-218
Hong, S.Y. 1,5; 669-678
1,5; 705-714
Hsu, C.-J. 1,3; 359-361
Hsu, I.-M. 1,3; 359-361
Hwang, W.-S. 1,5; 625-636
Hylton, T.A. 1,5; 609-613
Ikeda, D.E. 1,2; 211-218
Ito, T. 1,2; 211-218
Jackson, J.E. 1,3; 415-428
Jacobson, D.L. 1,5; 679-684
Jaffee, R.I. 1,2; 227-234
Jiles, D.C. 1,2; 249-253
Jordan, W.M. 1,2; 261-265
Kaminski, D.A. 1,2; 249-253
Kaneko, T. 1,1; 29-34
Kannan, D. 1,6; 801-812
1,6; 813-822
Kansal, U. 1,3; 393-398
Kassner, M.E. 1,3; 393-398
Katter, M. 1,2; 175-181
Khatak, H.S. 1,6; 823-830
Kim, I. 1,4; 555-564
Klinzing, W.P. 1,1; 49-60
Kotchman, D.P. 1,4; 555-564
Krause, A.R. 1,1; 67-74
Krauss, G. 1,5; 695-703
Kubota, T. 1,2; 219-225
Kuhrt, C. 1,2; 175-181
Kwon, S.C. 1,3; 353-358
Lee, D. 1,4; 555-564
Lee, G.H. 1,3; 353-358
Leep, H.R. 1,6; 797-800
Lehman, R.L. 1,4; 543-546
Leisk, G. 1,1; 45-48
Li, L. 1,2; 205-209
Li, W. 1,3; 409-413
Lin, K.-L. 1,3; 359-361
Liu, S. 1,2; 183-191
Lointier, P. 1,5; 637-649
Lucas, J.D. 1,6; 781-788
Luo, A. 1,6; 755-762
Luzzi, D.E. 1,2; 205-209
Majlessi, S.A. 1,2; 285-291
Martin, P. 1,4; 463-467
1,5; 615-624
Matlock, D.K. 1,5; 609-613
1,5; 685-693
1,5; 695-703
Matsev, A.T. 1,1; 9-10
Milián, J.L. 1,2; 275-283
Moses, A.J. 1,2; 235-244
Mudali, U.K. 1,3; 341-345
1,6; 831-838
Mudawar, I. 1,1; 49-60
Muller, D.E. 1,4; 489-493
Nagai, T. 1,2; 219-225
Nakamura, H. 1,2; 211-218
Nakashima, S. 1,2; 211-218
Narayanan, C. 1,6; 823-830
Narendranath, C.S. 1,5; 651-657
Nichting, R.A. 1,1; 35-44
Northwood, D.O. 1,1; 21-27
1,1; 143-148
Novikov, P. 1,1; 9-10
Ogren, J.R. 1,3; 297
1,4; 433
1,5; 577
Olson, D.L. 1,1; 35-44
Oppliger, S.J. 1,1; 129-142
Park, M.J. 1,3; 353-358
Patni, K. 1,1; 91-96
Paul, A.J. 1,5; 659-668
Pickles, C.A. 1,3; 317-322
Pitt, C.H. 1,2; 255-260
Polonis, D.H. 1,3; 371-382
Ponnappan, R. 1,6; 755-762
Putatunda, S.K. 1,1; 67-74
Qui, W.W. 1,1; 75-82
Radhakrishnan, V.M. 1,1; 123-128
1,3; 333-340
Raghavan, J. 1,1; 67-74
Rashidi, M. 1,3; 323-331
Rasty, J. 1,4; 547-554
Ray, E.A. 1,2; 183-191
Rivera-Dominguez, A. 1,2; 261-265
Rozzi, J.C. 1,1; 49-60
Sa, C.-Y. 1,4; 555-564
Saigal, A. 1,1; 45-48
Saito, Y. 1,6; 789-796
Salsgiver, J.A. 1,2; 151
Schmidt, N.B. 1,4; 483-488
Schnitzke, D. 1,2; 175-181
Schultz, S. 1,2; 175-181
Schuster, H. 1,3; 333-340
Schwerdtfeger, K. 1,3; 399-407
1,4; 565-571
Shaikh, H. 1,6; 823-830
Shi, L. 1,1; 21-27
Shivpuri, R. 1,4; 495-503
1,4; 505-516
1,4; 517-530
Singleton, E.W. 1,2; 193-203
Sipahi, L.B. 1,2; 249-253
Spalvins, T. 1,3; 347-351
Spis, A. 1,1; 67-74
Sridharan, K. 1,4; 489-493
Srikrishna, M. 1,3; 415-428
Stadelmaier, H.H. 1,2; 167-174
Sun, J. 1,4; 463-467
1,5 615-624
Sundar, M. 1,6; 831-838
Swisher, J.H. 1,1; 75-82
1,3; 399-407
1,4; 565-571
Taheri, A.K. 1,2; 285-291
Tan, Y.M. 1,1; 91-96
Taylor, R. 1,2; 245-248
Umezu, Y. 1,4; 543-546
Utsunomiya, H. 1,6; 789-796
Valin, F. 1,5; 637-649
Vallance, D.W. 1,5; 685-693
Van Karsen, C.D. 1,3; 363-369
Venkadesn, S. 1,6; 923-830
Venkatraman, M. 1,5; 651-657
Viana, C.S. Da Costa 1,6; 751-754
Vinod, N. 1,6; 831-838
Wall, R.N. 1,5; 679-684
Wallis, R.A. 1,6; 781-788
Walter, K.C. 1,4; 489-493
Wang, K.F. 1,1; 97-112
Wang, Y.Z. 1,2; 193-203
Ward, J. 1,6; 781-788
Watanabe, T. 1,6; 789-796
Wecker, J. 1,2; 175-181
Wenzloff, G.J. 1,5; 609-613
Werner, F.E. 1,2; 227-234
Wert, J.J. 1,1; 129-142
Whittenberger, J.D. 1,4; 469-482
Worzala, F.J. 1,6; 845-848
Wu, S. 1,3; 409-413
Yang, H.T.Y. 1,1; 97-112
Yashiki, H. 1,1; 29-34
Yeh, H.-L. 1,5; 625-636
Yelon, W.B. 1,2; 193-203
Zarzour, J.F. 1,5; 659-668
Zhang, Y. 1,3; 317-322
Zhao, Z. 1,5; 669-678
1,5; 705-714